Basement Geophysical Interpretation of the National Petroleum Reserve Alaska (NPRA), Northern Alaska - Part II, the Gravity Story

by R.W. Saltus[1], T.L. Hudson[2], and J.D. Phillips[1]

Open-File Report 01-0476
2001

1 U.S.Geological Survey, MS 964, Denver, CO (saltus@usgs.gov, jeff@usgs.gov)
2 Applied Geology, PO Box 1428, Sequim, WA (ageology@olypen.com)

Introduction

Three-dimensional spatial variations in subsurface rock density combine to produce surface gravity variations. We make use of extensive knowledge of the thickness and physical properties of Mississippian and younger rocks (from seismic interpretation and borehole studies) to calculate the expected gravity effect of these rocks. When this "basin gravity" is subtracted from the observed surface gravity the result is the predicted gravity effect of pre-Mississippian basement rocks.

On this poster we give a graphical account of the construction of this gravity model. In addition we display maps showing the predicted Moho depth and thickness of the lower crust in this region.

We interpret the resultant basement gravity map to indicate two contrasting basement density domains: normal and dense. The normal (average density) domain produces gravity values consistent with typical sialic crustal densities. The dense domain is consistent with the presence of significant amounts of denser material such as mafic rocks.

Location map

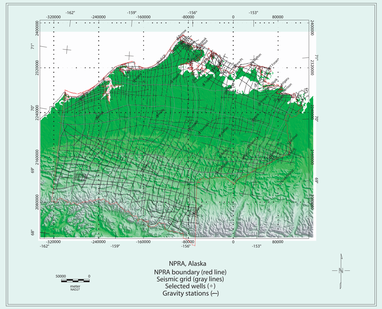

Project flowchart

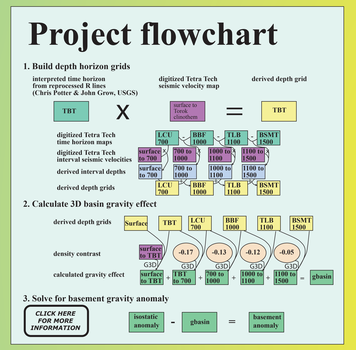

Model layers

CLICK HERE FOR MORE INFORMATION

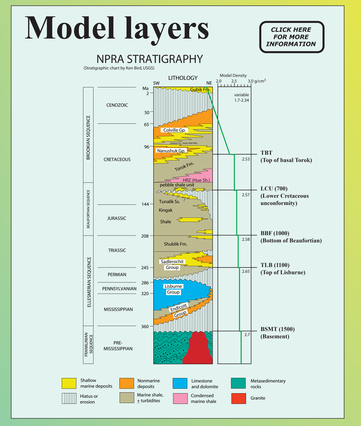

Depth layer stack- 3D views

CLICK HERE FOR MORE INFORMATION

1. Topography

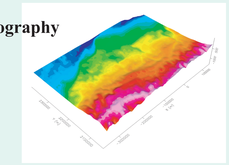

2. Top of basal Torok

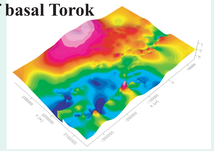

3. Lower Cretaceous Unconfomity

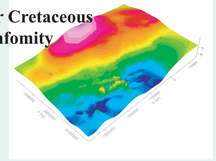

4. Bottom of Beaufortian

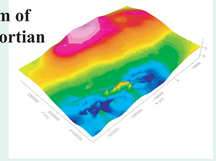

5. Top of Lisburne

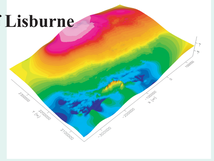

6. Basement

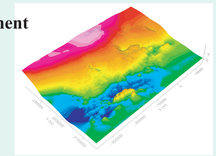

Gravity stack- 3D views

CLICK HERE FOR MORE INFORMATION

1. Surface to top of basal Torok

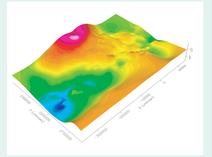

2. Top of basal Torok to lower Cretaceous unconformity

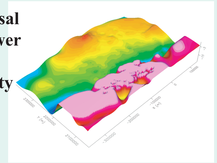

3. Lower Cretaceous unconformity to bottom of Beaufortian

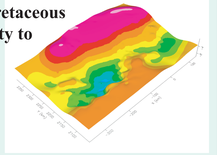

4. Bottom of Beaufortian to top of Lisburne

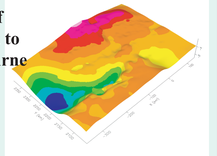

5. Top of Lisburne to basement

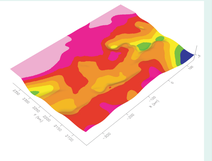

6. Surface to basement

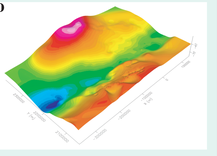

CBA Gravity

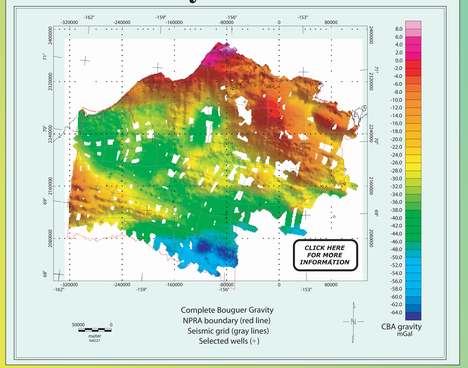

Isostatic Residual Gravity

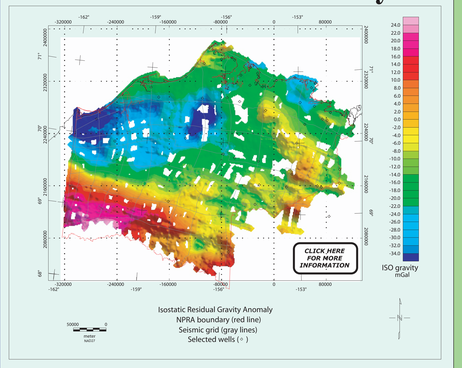

Basement Gravity

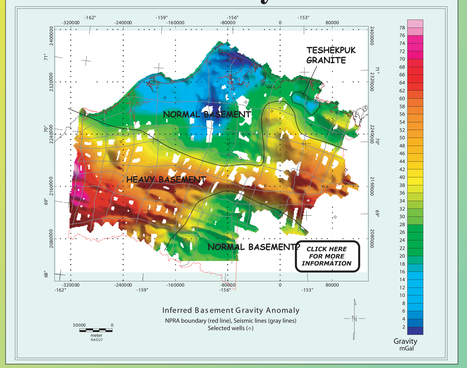

Isostatic Moho

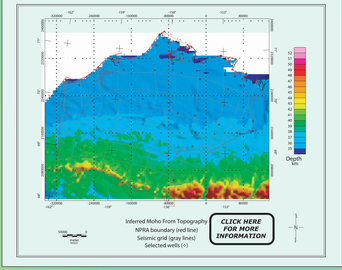

Basement Thickness

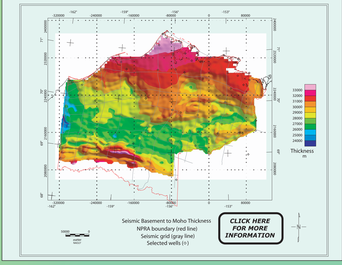

Conclusions/ References

Our gravity analysis yields some broad-scale observations about the basement in the NPRA region of northern Alaska. In the northern part of NPRA, the basement is thick (>32 km) and produces gravity anomalies consistent with normal sialic crustal densities. In the southern part of NPRA, the basement is thin (<26 km) and produces gravity anomalies consistent with a more mafic composition. Within the northern region, an elliptical basement gravity low surrounds the East Teshekpuk borehole. This low may define the boundaries of the basement granite body penetrated in the borehole. In the southern part of the study area, our gravity model is less reliable because of uncertainties relating to complicated thrusting.

Grye, George, (ed.), 1988, Geology and Exploration of the National Petroleum Reserve in Alaska, 1974 to 1982: U.S. Geological Survey Professional Paper 1399, 940 pp.

Parker, R.L., 1972, The rapid calculation of potential anomalies: Geophysical Journal of the Royal Astronomical Society, v. 31, p. 447-455.

Tetra Tech, 1982, Petroleum exploration of NPRA 1974-1981 (Final Report): Tetra Tech Report No. 8200 (including maps at 1:500,000 scale).

Weiland, W., 1989, An integrated approach to gravity anomaly separation by geologic stripping: M.S. Thesis, Colorado School of Mines, 168 pp.

CLICK HERE FOR MORE INFORMATION

http://geology.cr.usgs.gov/pub/open-file-reports/ofr-01-0476/

Basement Geophysical Interpretation of the National Petroleum Reserve Alaska (NPRA), Northern Alaska – supplementary text

By R.W. Saltus, T.L. Hudson, and J.D. Phillips

Open-File Report 01-0476
2001

TEXT TO ACCOMPANY BOXES ON POSTER PANEL 2 – Part II, the Gravity Story

Project flowchart

This box contains a pictorial representation of the steps involved in our 3D modeling of gravity data from the North Slope. The rectangles indicate data and are color-coded as follows: travel-time surfaces are blue-green, seismic velocities are purple, calculated interval depths are gray-blue, calculated interface depths are yellow, and gravity is green. Ovals depict uniform density contrast values based on borehole density logs. Lines between rectangles indicate data flow with the nature of combinatorial operations (subtraction, addition, multiplication) indicated by standard mathematical symbols. Geologic interfaces are labeled as follows (see NPRA stratigraphy in the Model Layers box on the poster): TBT = top of basal Torok, LCU = lower Cretaceous unconformity, BBF = base of Beaufortian, TLB = top of Lisburne, BSMT = seismic basement.

In step 1, grids defining depths to various geologic interfaces were prepared from digitized seismic interpretations and interval velocities. The TBT (top of basal Torok) depth interface was calculated by multiplying the interpreted time horizon (picks by Chris Potter and John Grow, USGS) by seismic velocities defined by Tetra Tech, Inc. (1982). The other interfaces were defined from information digitized entirely from Tetra Tech (1982) mapping. The seismic interfaces were digitized from travel time maps and the velocities from contour maps of interval velocities. Differences were calculated between seismic time intervals and these differences were multiplied by interval velocities to calculate interval thicknesses. The interval thicknesses were successively summed to calculate interface depths.

In step 2, the resulting depth interfaces from step 1 were used as upper and lower boundary grids for 3D calculation of the gravity effect for each seismic interval. For the interval from the surface to the top of basal Torok, interval densities were variable based on seismic velocities from Tetra Tech (1982) mapping. All other interval densities were constant values based on well data analysis by us and by Weiland (1989). We used an implementation of the Parker 3D algorithm (Parker, 1972) for calculation of the gravity effect for each model layer. The layers (represented by the green rectangles at the bottom of step 2) were then summed to produce the modeled gravity effect of the basin (gbasin).

In step 3, the modeled gravity effect of the basin (gbasin) was subtracted from the isostatic residual gravity anomaly (isostatic anomaly) to produce the predicted basement gravity anomaly (basement anomaly).

Model layers

The right column summarizes the density model used for calculation of the basin gravity effect. The greatest density contrast, and therefore the largest component to the gravity model, is in the shallowest layer that extends from the surface to the top of the basal Torok. For this layer we converted Tetra Tech (1982) seismic velocities to density using standard curves (Telford and others, 1982). For each of the deeper interfaces we used densities based on borehole logs as interpreted by Weiland (1989) and us. Density increases with depth in our model. The overall model is relatively insensitive to the shapes of the deeper layers because the density contrasts are relatively small at depth.

Depth layer stack – 3D views

This box shows a series of perspective views of the individual interfaces in the basin model. Views are from the southwest. All the layers reflect the extreme shallowing of basement toward the Barrow arch in the center of the northern part of the study area. Each view has the colors scaled to that view; the colors do not represent consistent depths from view to view. Warm colors (reds) indicate shallow levels of each interface; cool colors (blues) are deep levels.

Gravity stack – 3D views

This box shows a series of perspective views of the individual gravity effects of each layer of the basin model. Views are from the southwest. The gravity values are all negative reflecting the low densities of the layers relative to the assumed density of 2.7 g/cm^3 for basement. Warm colors (reds) indicate values near zero; cool colors (blues) show regions with large negative gravity values. The predicted gravity effect of the basin is smallest over the Barrow arch where the basement is shallowest. The largest gravity effects are predicted over the deep portions of the basin and, in particular, to the west where the top layer of the model (surface to top of basal Torok) is thickest. The color scales of these views are scaled to each view – they are not consistent from view to view.

CBA Gravity

This map shows the complete Bouguer anomaly (CBA) values for NPRA. CBA gravity represents the integrated gravity effect of all density variations from the surface to the Moho, with the direct effects of topography removed. Because of isostasy (the tendency of the Earth's crust to be thicker in regions of high topography), CBA gravity generally shows an inverse correlation with topography. This is the case here – the highest CBA gravity values generally occur along the coast and the lowest values fall over the high Brooks Range in the southernmost part of the map. The southwest portion of the map shows a gravity high that persists despite relatively high topography there. Similarly, the general increase in CBA gravity values from west to east over the central portion of the map persists despite the lack of a topographic trend in that direction. To remove the

correlation between topography and CBA gravity we apply an isostatic correction to produce the isostatic residual gravity anomaly (described in the next section).

Isostatic Residual Gravity

This map shows isostatic residual gravity anomaly values for NPRA. Isostatic residual gravity anomalies represent the integrated gravity effect of density variations in the upper crust (from the base of topography to the shallowest Moho). Application of the isostatic residual correction removes most of the correlation between topography and gravity that is present in CBA gravity (described above). Prominent isostatic anomaly features include the large gravity low in the northwest quadrant of the map, the mostly east-west trending gravity ridge in the southern portion of the map and the northwest-southeast trending gravity ridge in the eastern portion of the map. This map contains the combined effect of the gravity low from the sedimentary section and any density variation in the basement rocks.

Basement Gravity

This map shows the predicted gravity effect of basement rocks for NPRA. It is the result of subtracting the modeled gravity effect of the basin from the isostatic residual gravity anomaly. This map reflects density variations in the basement region – from the seismic basement interface to the shallowest Moho. The map is probably most sensitive to density variation in the upper portion of basement – deeper variations are likely to have been removed as part of the isostatic regional removal. We have drawn three basement gravity domains (described in more detail on poster panel I). Most of the basement gravity variation can be seen on the isostatic residual anomaly map as well. The exception is the southernmost "indeterminate basement" region. This feature of the basement gravity map is less robust than the other two domains because it is dependant on our assumptions of structure and physical properties in this deep and poorly known portion of the basin.

Isostatic Moho

This map shows a predictive model of the Moho based on gravity, topographic, and seismic data. We used a model of Airy isostasy (Airy, 1855; Simpson and others, 1986). In this model, the depth to the Moho is directly proportional to the longest wavelength features of topography. To fit the model to known Moho depths along the TACT seismic line (i.e., Fuis and others, 1997), we assumed a depth to Moho of 35 km at the shoreline, a topographic load density of 2.67 g/cm^3 (consistent with the Bouguer reduction density used above), and a density contrast across the Moho of 0.35 g/cm^3. This model predicts a steady increase in Moho depth as you proceed southward from the coast toward the topographic highs of the Brooks Range. The greatest depths to Moho are in the southern portion of NPRA where predicted depths exceed 40 km.

Basement Thickness

This map shows the predicted thickness of basement (defined here as that part of the lower crust between seismic basement horizon and the Moho). This thickness was calculated by subtracting the Tetra Tech seismic basement horizon from the predicted isostatic Moho. The basement portion of the crust varies by about 20% from a maximum thickness of more than 33 km in the Barrow region to a minimum of less than 26 km in the southwestern portion of NPRA. The basement is thicker than the minimum value in the southernmost part of NPRA because of basement-involved thrusting.

Conclusions/References – Poster panel 2

Our gravity modeling is based on some simplifying assumptions that deserve further discussion here. First, our models of interval density, while based on existing seismic velocity and borehole density information, are not well constrained, particularly for the deeper portions of the basin. However, we are very confident in the identification of the northern, "average density basement", and the southern, "dense basement", domains because these domains are also visible in the isostatic residual gravity data before application of modeling. Second, our model of the Moho is constrained by seismic data only along the TACT line at the very eastern portion of our map. We do not know exactly how isostatic compensation is achieved over the area as a whole. It is probable that there is some flexural rigidity to the crust and that there may be distributed isostatic compensation of the loading caused by Brooks Range thrusting. Distributed isostatic support would cause the Moho to be shallower under the Brooks Range than we have estimated – this would, in turn, increase the amount of predicted basement thinning in the south compared with our estimates.

REFERENCES CITED

Airy, G.B., 1855, On the computation of the effect of the attraction of the mountain-masses, as disturbing the apparent astronomical latitude of stations in geodetic surveys: Philisophical Transactions of the Royal Society of London, v. 145, p. 101-104.

Fuis, G.S., Murphy, J.M., Lutter, W.J., Moore, T.E., Bird, K.J., and Christensen, N.I., 1997, Deep seismic structure and tectonics of Northern Alaska; crustal-scale duplexing with deformation extending into the upper mantle: JGR, B, v. 102, n. 9, p. 20,873-20,896.

Parker, R.L., 1972, The rapid calculation of potential anomalies: Royal Astronomical Society of London Geophysical Journal, v. 31, p. 447-455.

Simpson, R.W., Jachens, R.C., Blakely, R.J., and Saltus, R.W., 1986, A new isostatic residual gravity map of the conterminous United States with a discussion on the significance of isostatic residual anomalies: JGR, v. 91, n. B8, p. 8348-8372.

Telford, W.M., Geldart, L.P., Sheriff, R.E., and Keys, D.A., 1982, Applied Geophysics: Cambridge University Press, New York, 860 pp.

Tetra Tech, 1982, Petroleum exploration of NPRA 1974-1981 (Final report): Tetra Tech Report No. 8200, Tetra Tech, Inc., Pasadena, California.

Weiland, W., 1989, An integrated approach to gravity anomaly separation by geologic stripping: M.S. Thesis, Colorado School of Mines, 168 pp.